electronics

MDPI

Article

Power System Inertia Estimation Using Hybrid PSO-GA in Grid-Scale Energy Storage Systems

Mohamed Farah Abdilahi and Yunus Yalman *

Faculty of Engineering and Natural Sciences, Ankara Yıldırım Beyazıt University, Ankara 06010, Türkiye; 225105124@aybu.edu.tr

* Correspondence: yunusyalman@aybu.edu.tr or mhmdfrh.krye@gmail.com

Abstract

The increasing penetration of renewable energy technologies such as wind and solar photovoltaics has displaced conventional synchronous generation, resulting in reduced system inertia. Low-inertia conditions degrade frequency stability and limit the power system's disturbance response capability. Accurate inertia estimation is therefore essential to prevent over-frequency events, unintended protection actions, load shedding, and cascading failures. Moreover, the variability of renewable energy sources complicates inertia dynamics, rendering traditional approximation-based estimation methods inadequate for modern power systems. This paper proposes a novel hybrid optimization-based inertia estimation method that combines particle swarm optimization (PSO) and genetic algorithm (GA) for grid-scale energy storage systems. Unlike conventional approaches, the proposed framework systematically integrates inertia formulations applicable to both synchronous generators and converter-interfaced resources within a unified estimation structure. The performance of the proposed method is evaluated and compared with PSO and GA using the IEEE 39 bus system in two disturbance scenarios. The results demonstrate that the proposed hybrid PSO–GA approach achieves superior robustness, estimation accuracy, and adaptability for operational inertia awareness and near real-time inertia applications. The results confirm that the proposed method provides an effective and reliable inertia estimation tool to support frequency regulation, enhance disturbance response, and ensure secure operation of low-inertia power systems.

Keywords: power system inertia estimation; low-inertia power systems; hybrid PSO–GA optimization; battery energy storage systems (BESS); synthetic inertia

Check for updates

Academic Editor: Francisco Javier Ruiz-Rodríguez

Received: 27 January 2026
Revised: 27 February 2026
Accepted: 27 February 2026
Published: 2 March 2026

Copyright: © 2026 by the authors. Licensee MDPI, Basel, Switzerland. This article is an open access article distributed under the terms and conditions of the Creative Commons Attribution (CC BY) license.

1. Introduction

The increasing incorporation of renewable energy sources like wind and solar photovoltaics is replacing conventional synchronous generators for reducing carbon dioxide emissions and achieving environmental gains [1]. However, this transition poses major difficulties for grid stability, especially with regards to the fact that the inherent reduction in system inertia as converter-interfaced generators substitutes synchronous generators [2]. The reduced inertia, which is a paramount parameter of power systems' capacity to support the decreased frequency variations, requires improved methods of estimation to guarantee grid stability and operative security [3]. Accurate inertia estimation is critical to prevent unintended over- and under-frequency relay operations, load shedding, and cascading failures [3].

The time-varying nature of renewable energy sources further complicates inertia estimation, as system inertia itself becomes a time-dependent parameter that must be continuously and accurately monitored [2,4]. This increased complexity highlights the need for advanced real-time inertia estimation techniques, including recursive algorithms, capable of tracking rapidly changing system dynamics and enhancing grid reliability [3]. Furthermore, the emergence of wide-area measurement technologies enables continuous monitoring of system inertia and supports the assessment of virtual inertia contributions from converter-interfaced generation units [2,3].

Inertia estimation techniques have become a critical aspect of frequency stability assessment, particularly as power systems increasingly rely on inverter-based renewable energy sources and fast power electronic controls. As reported in [5], inertia can no longer be regarded as a fixed system parameter but rather as a time-varying quantity influenced by the generation mix, operating conditions, and disturbance characteristics, with existing approaches categorized into offline-, online-, and forecasting-based methods. Building on this perspective, [6] further highlights that low-inertia operation introduces additional challenges related to system observability, noise sensitivity, controller interactions, and the growing influence of synthetic inertia and fast frequency response from converter-interfaced resources. Collectively, these studies demonstrate that inertia estimation in modern power systems is inherently more complex than in traditional synchronous-dominated grids, despite advances in computational capability and measurement quality.

Several recent macro surveys have been done investigating the issue of inertia estimation within the current low-inertia power systems [2,3,5,6]. These group the inertia estimation algorithms into two general types: model-based algorithms (in which the modeling of the system is made and known parameters of the machine are used) and measurement-based algorithms (in which data on disturbances or responses are used). Most of the reviews also record the shift to data-driven (AI-assisted) methods and even strategies based on optimization in determining inertia [7,8]. In [9], methods are classified according to their temporal characteristics—namely, offline post-mortem analysis, online real-time estimation, and forecasting—reflecting the growing concern for inertia prediction as the power grid continues to evolve. In fact, it is now considered necessary to predict inertia with accuracy for hours or days to come to be able to schedule rapid frequency reserves in the renewable-intensive system [9,10]. In all these surveys, the general conclusion is that the conventional techniques are severely constrained when penetrations go high in renewable and BESS.

It is common to find that model-based inertia estimation techniques are becoming less accurate as the system inertia of variables approaches, and that this inertia somewhat conceals the dynamics of converter interface resources [2–5]. The fact that physical inertia is decoupled from the grid frequency response, which can be attributed to these resources, limits the applicability of traditional modeling assumptions and undercuts the reliability of all model-based methods [2–4,6]. In comparison, the current practice of measurement-based inertia estimation techniques is mostly based on significant disturbance events in order to infer system inertia, although such disturbances are unlikely to recur in highly distributed and actively controlled power systems. In turn, the fact that it relies on system-wide disturbances, which occur only periodically, puts an extra burden on the viability and sustainability of these measurement-based methods in the modern low-inertia grids [8].

Most online inertia estimation tools use dispatch-based methods to sum, often forgetting inverter-based and demand-side response inertia contributions, while many measurement-based tools do not model virtual inertia due to battery energy storage or demand-side response [2,5]. This method underestimates inertia in low-inertia situations. The proposed recent literature suggests probing methods, i.e., the active injection

of minor disturbance signals through controllable inverters to measure the system inertia time-varyingly and refined continuous estimation and AI solutions to close these gaps [11]. Active probing indicators and inertia predictors significantly facilitate the situational awareness of grid frequency stability [9,11]. These studies propose more flexible inertia estimation methods to deal with the difficulty of high renewable penetration and energy storage integration [8].

In [5,6], most of the inertia estimation methods have their roots in swing equation-based interpretations of the initial frequency dynamics, and result in the rate of change of frequency (RoCoF)-based and disturbance-based methods. Although these methods appear attractive in terms of transparency and ease of physical implementation, both [5,6] specify their inefficacy in situations of high renewable penetration, including increased sensitivity to measurement noise. In addition to that, reliance on correct timing, magnitude of disturbances, and failure to separate the effects of inertia on damping, governance response, and load frequency dependence are other problems addressed in those studies. Later improvements, including polynomial fitting [12], window-based estimators [13,14], and the usage of Kalman filters [15,16] would make it more robust, but further depend on parameter tuning, model fidelity, linearity, and the presence of wide-area measurements. However, more recent methods of identification and data-driven methods, including ARMAX models [17], stochastic estimation [18], deterministic WLS [19], artificial intelligence [20,21], machine learning [22]-based solutions, and active perturbation [23], reduce the need to explicitly define the disturbances and can continue to be estimated. Yet, they are limited by the needs of data, computational complexity, problems of generalization, and poor interpretability, especially where BESS, renewable generation and converter controls change quickly.

More recently, optimization-based techniques of inertia estimation have been introduced, including PSO and snake optimization (SO) methods, augmented with fine-tuned swing equations [24–26]. Yet, like before, they are prone to practical and system inference limitations, require detailed system models, and are disturbance-dependent and use known offline disturbances. Moreover, a literature review indicates that no reported cases exist where a hybrid PSO-GA framework has been used to estimate inertia in the presence of an integrated RES and BESS. As such, a concise overview of the literature methods that were discussed, as well as the description of their respective limitations, is depicted in Table 1.

Table 1. Summary of existing power system inertia estimation methods and their key limitations.

Reference	Technique Keywords	Main Inputs	Advantages	Disadvantages
[12]	Load power change after disturbance, inertia estimation	Frequency, load power change	Practice, event-based, limited model reliance	Event-dependant, sensitive to measure noise, disturbance charactization
[13]	Synchrophasor-based inertia estimation (GB system)	Synchrophasor frequency/phasors	PMU-based, system-level estimation	PMU coverage/quality dependence, assumptions made on disturbance and aggregation
[14]	Observed frequency transients, WECC equivalent inertia	System frequency transients	Uses real disturbances, bulk-system inertia	Disturbance-dependent, separation of effects (governor/load) difficult

Table 1. *Cont.*

Reference	Technique Keywords	Main Inputs	Advantages	Disadvantages
[15]	Data-driven adaptive inertia estimation, Unscented Kalman Filter	PMU streams, state estimation	Online tracking, noise-robust filtering	Requires model structure/tuning, computational cost, sensitivity to initialization
[16]	Sensitivity to disturbance time, event-based inertia estimation	Frequency event record	Highlights timing uncertainty, impact Method hygiene	Strong dependence on correct timing of event High risk of amplifying error
[17]	ARMAX-based inertia estimation using synchrophasors	Synchrophasor measurements, input-output data	Data driven, better noise handling than raw derivatives	Model order/tuning, data window requirement, convergence sensitivity
[18]	Precise RoCoF estimation algorithm (for inertia inference)	High-rate frequency/PMU	Improved RoCoF quality, supports event-based inertia	Still derivative-sensitive, filtering/latency trade-offs
[19]	Center-of-inertia frequency, Real-time inertia computation	Multi-location frequency, COI aggregation	Wide-area suitability, Real-time potential	COI formulations assumptions, Measurement Synchronization requirements
[20]	ANN-based inertia estimation	Training data, measurements/features	Fast inference, nonlinear mapping	Data-hungry, generalization risk, black-box interpretability
[21]	Dual-stage hybrid deep learning ensemble (LSTM-MLP, TCN-LSTM, ConvLSTM), bias–variance reduction	Mechanical power (Pm), electrical power (Pe), RoCoF, PV power, te PMU-like data	High real-time accuracy, robust under multiple operating conditions, xxplicit RES integration, scalable to larger systems	Data-intensive training, high computational training cost, black-box nature, sensitive to RoCoF/PV noise
[22]	ML-assisted inertia estimation from ambient measurements	Ambient PMU data	Continuous estimation, no large disturbance required	Feature/model drift, data quality dependency, validation complexity
[23]	Small power injection test, synthetic inertia estimation/demonstration	Controlled injection + measurements	Works without major faults, inverter/BESS-friendly concept	Practical deployment constraints, signal design, local vs system-wide inference limits
[24]	PSO, optimization-based, frequency model fitting	Frequency response, system parameters, disturbance data	Accurate estimation, global search, nonlinearity handling	Requires detailed system models, offline use, no explicit RES/BESS modeling

Table 1. *Cont.*

Reference	Technique Keywords	Main Inputs	Advantages	Disadvantages
[25]	Snake Optimization Algorithm (SO), improved swing equation (linearized frequency and voltage factors)	Frequency and voltage deviations, known disturbance magnitude	Transient-aware, high accuracy, global convergence	Complex model, disturbance-size dependency, offline use, needs known disturbance size
Proposed Method	Hybrid PSO global + GA local tuning, physics-informed optimization, RES + BESS integrated	Frequency response, power signals, IEEE 39 bus simulation/PMU-like data	Optimum search + local refinement, explicit RES and BSS integration, flexible objective design	Computation time, metaparater tuning, depends on the fidelity of model/data used for fitness

This paper introduces a novel hybrid PSO–GA-based methodology for accurate inertia estimation in power systems with integrated energy storage systems and renewable energy sources using the modified IEEE 39 bus system. The aim is to enhance the precision and dependability of the inertia measurements in contemporary power networks. This design is suggested as the immediate answer to the identified gaps in the above reviews. In contrast to traditional methods of analysis (based on simplified modeling or steady-state assumptions) or black-box AI predictors (based upon vast training layers and potentially opaque), the given approach takes advantage of metaheuristic optimization to comprehend the inertia constant in a physics-informed fashion. Specifically, the PSO-GA hybrid algorithm is effectively used to search for the inertia values that can most effectively explain the mechanics of a system, thus removing the limitations of local or linear estimation principles. The innate difference of this estimator from the current methods is that it is an optimization-based estimator that simultaneously considers the effect of the inertia of the synchronous generators, the inverter-based resources, and the BESS units in a single model. It provides a direct statement to the unrestricted problem of measuring and tracing the synthetic inertia of converter interface resources. The technique can capture multi-source inertia behavior that may be overlooked in analyses based on analytical formulas or dispatch estimates by tuning a detailed system inertia model to measure data. This is attributed to the ability of the PSO–GA metaheuristic to efficiently explore the complex and nonlinear search space, providing global optimization capabilities while overcoming the inaccuracies of conventional identification methods and improving robustness to measurement noise and model uncertainties. As a result, the suggested hybrid solver provides a high-fidelity inertia prediction that is highly valid for the low-inertia, highly dynamic systems. It can be adapted to changing inertia conditions and enables the system operators to use real-time and comprehensive inertia information. This work addresses a critical gap in the literature by providing a powerful framework for estimating the overall system inertia in power systems where both conventional and virtual inertia sources coexist. Finally, the proposed PSO–GA-based approach advances the state of the art by effectively combining model-based designs with computational intelligence, enabling reliable inertia assessment in next-generation power grids. Nevertheless, in one case, a hybrid PSO-GA predicted an inertia constant of 4.49 s, which closely matched the actual system inertia of 4.5 s and another 4.11 s with an actual inertia of 4.10 s. By contrast, PSO and GA overestimated the inertia constant, producing values of 4.62 s and 4.67 s in Scenario 1 and 4.18 s and 4.23 s in Scenario 2 respectively. These results show that the proposed hybrid PSO-GA (HPSO) framework provides superior estimation accuracy and robustness, particularly in the presence of BESS-induced fast frequency dynamics.

The contributions of this paper can be summarized as follows:

- Development of a novel hybrid PSO-GA framework for inertia estimation in power systems with grid-scale BESS, ensuring high accuracy under converter-dominated operating conditions by leveraging the complementary global and local search capabilities of both algorithms.
- Proposal of a unified inertia estimation model that integrates both physical rotating inertia and synthetic inertia contributions from BESS into a single, cohesive mathematical representation.
- Implementation of a graded inertia control strategy that facilitates controlled and constant variations in system inertia, providing a robust benchmark for evaluating the precision of estimation methods.
- Formulation of a multi-metric optimization objective that incorporates both frequency trajectory and RoCoF properties to enhance estimation reliability.
- A comparative analysis demonstrating the superior precision, convergence, and numerical stability of the hybrid PSO-GA approach relative to standalone PSO and GA techniques in two different scenarios.

The remainder of this paper is organized into five core sections. Section 1 introduces the challenges of inertia estimation in modern low-inertia power systems and provides a comprehensive literature review of existing methodologies. In Section 2, the methodology is detailed, covering the unified system modeling and the proposed hybrid PSO-GA framework, alongside the study setup involving the IEEE 39 bus system, case studies and grid-scale BESS integration. Section 3 presents the results, evaluating the performance of the hybrid approach in comparison with standalone PSO and GA methods and their practical implications for grid stability. Finally, Section 4 concludes this paper by summarizing the key contributions and suggesting directions for future research.

2. Methodology

This section outlines a unified scheme for the description of system frequency and inertia, and it starts with the basic formulation of the swing equation and its application to the description of electromechanical dynamics in perturbation. It then reviews optimization-based inertia estimation procedures and outlines the test system model that is chosen to model the dynamic behavior of a synchronous generator as well as the grid-scale battery energy storage system. On the basis of this, the hybrid PSO-GA approach is elaborated as a powerful estimation approach that integrates global searching features with refinement to adapt to the variability of inertia in converter-dominated power systems. The final part summarizes the way in which the proposed methodology is adapted to effectively estimate effective system inertia in a range of operating conditions and perturbation conditions.

2.1. Power System Inertia

An accurate assessment of the power system inertia is essential for the proper control of frequency and stability analysis, particularly since the role of the traditional synchronous generators is eroded and the inverter-based resources become more prominent [27,28]. In this changing environment, inertia can loosely be defined to both synchronous generators and converter-interfaced generators, and unique estimation approaches are required for each type [2]. Although model-based methods of synchronous generators may typically exploit swing equations, their use with converter-interfaced generators is restrained by both the uncertainty of their control strategy and by the lack of replicated dynamics [2]. Recent developments indicate that the control systems may replicate the dynamic behavior of synchronous machines, thus allowing virtual inertia implementation in resources based on inverters [27]. This notion is critical for frequency deviation reductions in power networks

with high levels of converter-based generators; it enables the resources to play an active role in frequency correction, even in the case when such resources do not have an inbuilt rotational mass [29].

In such a way, the system inertia has become the inertia of the mechanical machines in addition to the synthetic inertia of inverter-based resources that are now well-controlled [29]. Additionally, the effective inertia of a power system, which considers the interaction between a change in power balance and the speed of change of frequency, is not limited to the conventional contributions of spinning mass but also includes the contributions of loading dependency and power electronic interfaces to the inertia [30,31]. This detailed description illustrates the necessity of employing estimation methods that can precisely measure all the elements of physical and virtual inertia in a variety of generation technologies, including energy storage devices of a grid scale [2]. The full cognizance of inertia is essential in the development of correct estimation methodologies for the varying and changing effects of modern power system components [11]. Such approaches cannot be done without describing the spatiotemporal distribution of inertia, which is constantly varying as a result of the operating state of the system and the dynamic virtual inertia emulation of converter-interfaced generators [2,30]. This complexity, in turn, requires an overhaul of the conventional inertia estimation models and an advancement towards more simplistic models to take into consideration the dynamic response of rapid acting controls and energy storage technologies of grid scale [11,22].

2.2. Response Frequency and Inertia

The relationship between frequency response and inertia is found in the dynamic behavior of the power systems following a disturbance. Particularly, the first order of change in frequency is inversely proportional to the total inertia of the frequency changes in power systems following a disturbance such as a generator fault observed in multiple cycles, as illustrated in Figure 1. The primary inertial response (A—grey-shaded region) is that of the synchronous generators, when the stored kinetic energy is discharged to compensate for the loss of power; this is important in reducing the lowest frequency point and the ROCOF. The lowest frequency in the transient period is the frequency nadir [32]. This is followed by a secondary response phase (B—green-shaded region), which is a controlled reaction to further smooth frequency variations.

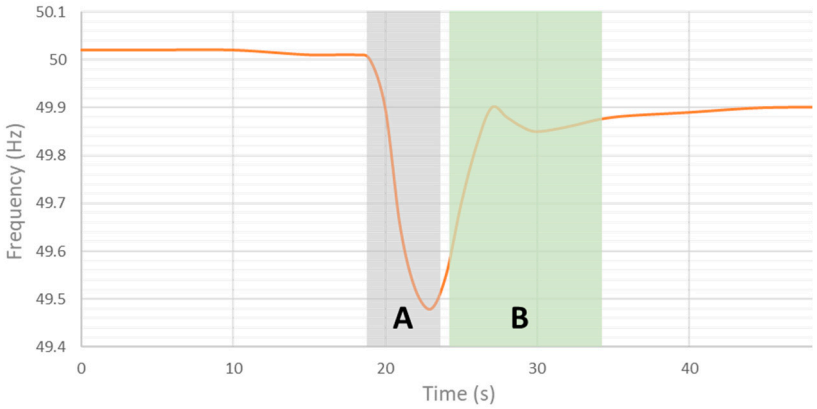


Figure 1. Frequency control phases in power systems.

The main factor that contributes to rotating inertia, the determinant of inertial response, is the generators and turbines present in synchronous generators. When a disturbance occurs, an unbalanced torque is exerted on the synchronous generator's rotors and they either accelerate or decelerate. The swing equation of the *i*th synchronous generator

considered in a power system, and the angular momentum of the nth generator are given in Equations (1)–(3).

$$M_i \frac{d^2\delta_i}{dt^2} + D_i \frac{d\delta_i}{dt} = P_{m,i} - P_{e,i} \tag{1}$$

$$M_i = \frac{2H_i}{\omega_s} \tag{2}$$

$$\frac{2H_i}{\omega_s} \frac{d^2\delta_i}{dt^2} + D_i \frac{d\delta_i}{dt} = P_{m,i} - P_{e,i} \tag{3}$$

where the rotor angle of the nth generator, denoted by δ_i, is expressed in electrical radians (or degrees), while t represents time in seconds. The parameter M_i denotes the angular momentum of the nth generator, typically expressed in per unit or in MJ·s per electrical radian, and H_i is the corresponding inertia constant, commonly given in MJ/MVA or seconds. The synchronous angular speed is represented by ω_s in rad/s. The damping coefficient of the nth generator is denoted by D_i, accounting for the damping torque that arises due to slip speed-dependent effects. The mechanical input power supplied by the prime mover of the nth generator is represented by $P_{m,i}$ (pu), whereas $P_{e,i}$ denotes the electrical power output delivered to the grid (pu). The accelerating power $P_{a,i}$, defined as the difference between mechanical and electrical power, is given by $P_{a,i} = P_{m,i} - P_{e,i}$ in per unit.

Swing Equation

The swing equation, which is commonly considered the basic dynamic model used in estimating inertia in power systems, is a simplified second-order differentiation of the generator rotor dynamics to power imbalances. Although this has made it a popular tool for offline inertia estimation due to its clarity and physical interpretability, its application to current power systems has been pointed out to be limited by various studies. The first is its abundance of assumptions regarding constant mechanical input and constant damping, which can hardly be true in systems with high penetration of inverter-based resources or responsive loads [2,7]. In addition, the swing equation requires post-disturbance frequency data that are accurate and the disturbance magnitude that is known, which is not easily available and can not be easily measured in practice [33–35]. As pointed out by [2,7], swing equation-based techniques are especially susceptible to error in the instances of noise, model uncertainty and unobserved frequency control interactions. When BESS or RES are used to provide synthetic inertia due to fast frequency controls, the fundamental swing model does not explain these very time-varying and controller-specific effects and so the inertia values given by it are often biased or non-representative of actual system behavior [2,9]. This implies that, although the swing equation is analytically tractable, serious augmentation or replacement is needed to perform proper estimation of inertia in low-inertia and renewable dominated grids.

The swing equation can be expressed in the form of rotor speed ω or frequency deviation Δf in:

$$2H \frac{d\omega}{dt} = P_M - P_e - D\Delta\omega \tag{4}$$

where H represents the inertia constant of the synchronous machine in the equivalent system, expressed in seconds. The variable ω denotes the rotor speed in rad/s, with the speed deviation defined as $\Delta\omega = \omega - \omega_s$, where ω_s is the synchronous speed. The mechanical input power is denoted by P_M (pu), while P_E represents the electrical output power (pu). The parameter D corresponds to the damping coefficient, expressed in per unit per rad/s, accounting for speed-dependent damping effects in the system.

The inertia constant (H), which is traditionally measured in joule seconds (Js) or watt-squared seconds (Ws^2), is a direct measure of the angular momentum of a generator or its stored kinetic energy. The formulation only describes the correlation between the kinetic energy of rotating parts and the internal power imbalance of the system [30]. On the other hand, the angular velocity of the rotor is calculated using the moment of inertia (J). The dynamic relationship that governs it is swing Equation (4), which can be obtained according to the second law of Newton and, therefore, describes whether an electric power network will oscillate or not [33,34]. Moreover, the power rating refers to the time that a generator needs to sustain its nominal power output and to counter the kinetic energy stored. In line with this, the inertia constant (H) is stated as a ratio of the stored kinetic energy of the generator to its rated rotational speed [9].

The rotor dynamic behavior of a single machine is frequently characterized by normalized constant inertia and a constant damping [27]. The dynamics of every synchronous generator in many machines tend to depend on the center of inertia. This enables one to achieve the equivalent system inertia, which is a result of the interacting dynamics of the individual machines [34]. The swing equation represents the relationship between power and frequency following a power mismatch. When applied to a single generator or an area of similar size, it is given in Equation (5).

$$\frac{\partial f_i}{\partial t} = \frac{P_i M - P_i E}{2 H_i S_{in} f_n} \tag{5}$$

where $P_i M$ denotes mechanical power, $P_i E$ denotes electrical load power, f_n is electrical frequency, H_i denotes inertia constant and S_{in} denotes nominal apparent power [35]. This equation indicates that the frequency change rate is directly proportional to power imbalance, and inversely proportional to the inertia constant, as well as the nominal apparent power [4,11].

2.3. Optimization-Based Methods

The techniques commonly used in these methods include recursive least squares or Kalman filters to estimate the time-varying aggregated inertia, which is an important component of systems where wind or photovoltaic power integration is large due to the unreliability of small generators [15]. Recent studies have further demonstrated the effectiveness of hybrid and data-driven optimization techniques for nonlinear system parameter estimation [35]. Ref. [36] proposed a hybrid swarm-based optimization framework that significantly improves convergence robustness in complex engineering systems, while ref. [37] employed advanced metaheuristic optimization for better convergence, stability and decision-oriented parameter estimation under uncertainty. These findings further motivate the adoption of cooperative hybrid optimization strategies for power system inertia estimation.

In addition, grid-scale energy storage systems, which are flexible systems, both as a controllable load and a generation source, add further complexity that provokes the use of sophisticated optimization-based inertia estimation techniques. These techniques are especially beneficial since they can explicitly model the behavior of bidirectional power flow and the time-varying behavior of virtual inertia emulation. Through the development of inertia identification about the system power imbalance that is measured in terms of the total injected power and the subsequent frequency response, optimization-based methods offer a perspective, sound and physically valid framework over the reliable estimation of system inertia during dynamic operating conditions [2,38].

2.3.1. Particle Swarm Optimization

PSO provides a reliable method of estimating inertia through simulating the social patterns of the bird flocks or fish schools; here, particles respond to their individual best-known positions as well as the group best position in a multi-dimensional search space, as depicted in Figure 2. This optimization approach is especially suited to complex and nonlinear issues, like inertia estimation, where analytic solutions of such problems are difficult to find, since the interaction between multiple system parameters and the variability of renewable sources of energy is dynamic in nature [9]. The particles are initially positioned in the state space randomly.

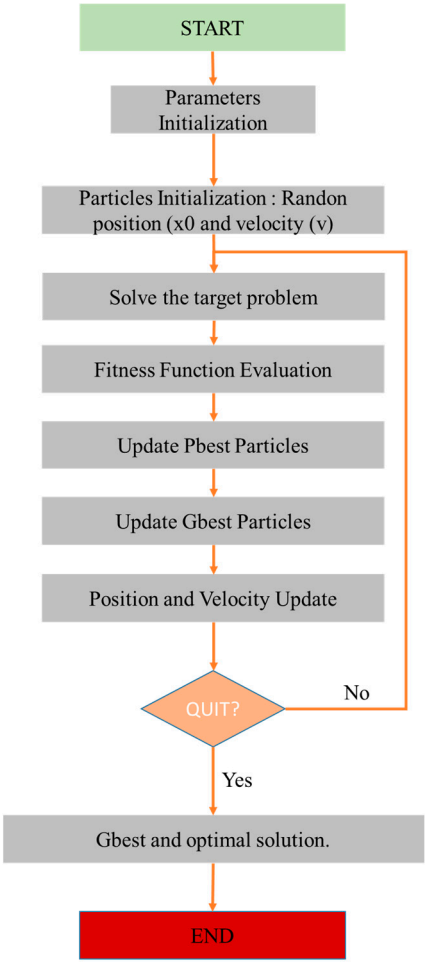


Figure 2. PSO algorithm flowchart.

The system therefore adjusts and applies its best known information, speed at the moment, and most profitable previous experiences of the swarm. The approach does not depend on local minima and instead takes advantage of the information within the state space [39]. In addition, the PSO algorithm, for being able to function efficiently without any knowledge of the gradient, is especially flexible in those cases when the systems under consideration can be characterized as either incomplete or strongly nonlinear, which is a common property of the present-day power grids that involve a wide range of different technologies in generating energy, as well as employing intricate control algorithms [40].

2.3.2. Genetic Algorithm (GA)

Genetic algorithms are an efficient optimization technique that relies on the laws of natural selection and genetics, commonly applied to complex issues in power systems,

including inertia calculation. The functionality of these algorithms is that they generate a pool of potential solutions in the form of chromosomes. They regulate such processes as selection, crossover and mutation to refine the solutions progressively through generations [41]. This evolutionary strategy enables genetic algorithms to explore a vast space of potential solutions very fast and as such are especially useful at maximizing power system stabilizers and in dealing with nonlinear dynamics associated with estimating inertia [42]. They are highly applicable to problems whose system model functions are complicated or computationally expensive, since they are able to find solutions that are proximate to the best possible without necessarily knowing how the objective functions vary. Moreover, genetic algorithms are also parallelizable, which is quite an asset to large-scale power systems where the efficiency of computation is vital. This provides them with a clear advantage over those gradient-based techniques, which may be computationally costly [43]. In addition, scientists are also considering hybridization approaches that can be used to address problems such as early convergence and stagnation that may diminish the quality of output of one metaheuristic algorithm [44]. Figure 3 depicts the general GA flowchart, starting with the step of initializing a population of candidate solutions, moving on to the fitness evaluation process, and then to the evolutionary operators of selection, crossover, and mutation. These cycles are repeated until the desired convergence criteria are achieved, thus providing an optimally refined solution.

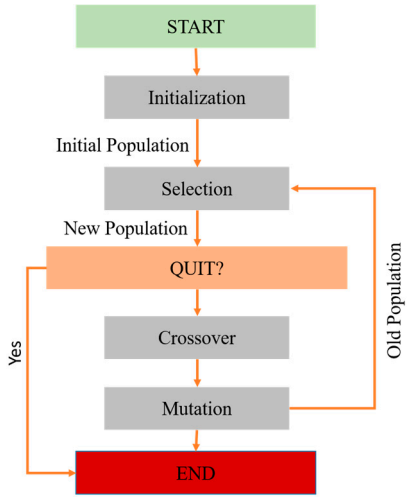


Figure 3. Genetic algorithm flowchart.

2.4. Test System

The New England system, a modified version of the IEEE 39 bus test system, is the basis for the analyses performed in this study. The original network has 10 synchronous generators, 39 buses, 46 transmission lines and 19 load points, and a base system capacity of 100 MVA, as shown in Figure 4. Details of power generation and demands for modified IEEE 39 bus systems are given in Table 2. The system model is developed and implemented in MATLAB 2021a using the Simulink environment, where the dynamic behavior of the test system and its components are modeled. This is designed to simulate the dynamic and transient behavior of a large interconnected power grid. The benchmark test system is often used for the evaluation of stability, reliability and control because of its balanced complexity that allows for computational efficiency, while still representing realistic power system dynamics. The network is a reduced representation of the interconnected New England and New York grids, but it essentially captures key dynamics such as rotor angle stability, frequency response and power transfer characteristics during a fault and contingency scenario. Its architecture lends itself to the evaluation of complex optimization and control

algorithms and is thus suitable for studies of grid operation, the integration of energy storage and the better integration of renewable energy sources.

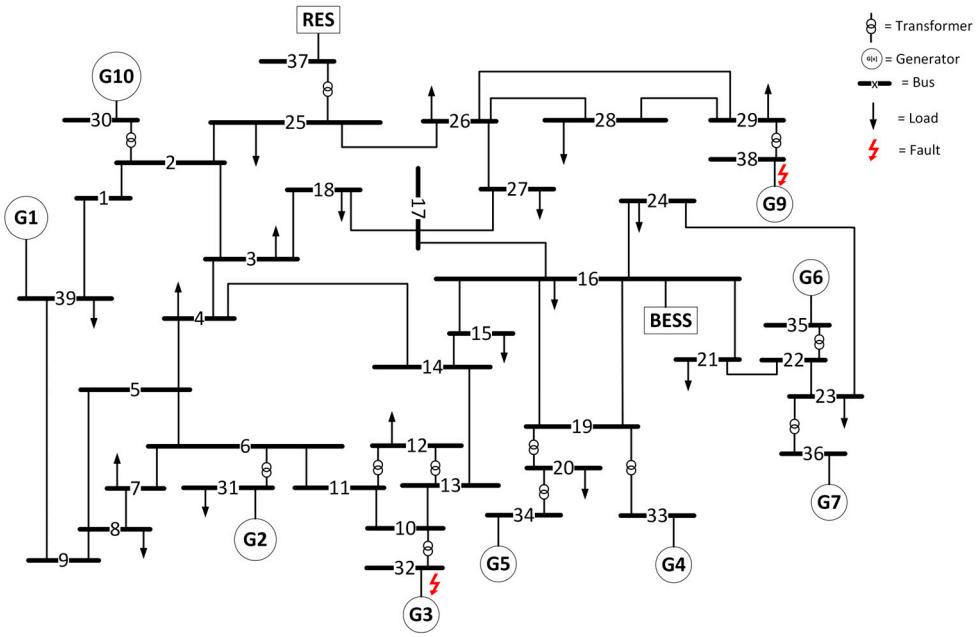


Figure 4. Test system single-line diagram.

Table 2. Active power generation (Pg) and power demand (P) distribution of the modified IEEE 39 bus system.

Bus No.	Bus Type	Generator	Pg (MW)	Pd (MW)	Note
3	PQ	---	0.0	322.0	---
4	PQ	---	0.0	500.0	---
7	PQ	---	0.0	233.8	---
8	PQ	---	0.0	522.0	---
12	PQ	---	0.0	7.50	---
15	PQ	---	0.0	320.0	---
16	PQ	---	0.0	329.0	BESS
18	PQ	---	0.0	158.0	---
20	PQ	---	0.0	628.0	---
21	PQ	---	0.0	274.0	---
23	PQ	---	0.0	247.5	---
24	PQ	---	0.0	308.6	---
25	PQ	---	0.0	224.0	---
26	PQ	---	0.0	139.0	---
27	PQ	---	0.0	281.0	---
28	PQ	---	0.0	206.0	---
29	PQ	---	0.0	283.5	---
30	PV	G10	250.0	0.0	---
31	PV	G2	323.0	9.2	---

Table 2. *Cont.*

Bus No.	Bus Type	Generator	Pg (MW)	Pd (MW)	Note
32	PV	G3	362.5	0.0	Fault—Scenario 2 (Scenario 1 + Scenario 2)
33	PV	G4	326.0	0.0	---
34	PV	G5	254.0	0.0	---
35	PV	G6	343.5	0.0	---
36	PV	G7	290.0	0.0	---
37	PV	RES	282.0	0.0	RES (PV)
38	PV	G9	432.5	0.0	Fault—Scenario 1
39	PV	G1	520.0	1104.0	Slack Bus

The incorporation of inverter-based generation requires adding or replacing a synchronous generator with PV generation while taking care of the stability of the system. An analysis of the inertia contribution from all the generators shows that generator 8 at bus 37 offers a small contribution to the total inertia of the system. Consequently, the replacement of this generator is accompanied by a small decrease in the equivalent inertia, which is enough to change the frequency dynamics without an excessively high RoCoF or loss of synchronism. The photovoltaic plant is modeled as a grid, following an inverter-based resource operating at a unity power factor. The steady state active power output is adjusted to match that of the replaced synchronous generator and hence maintains the power balance that existed before the disturbance. The photovoltaic unit is simulated without synthetic inertia and without quick frequency response, so that afterwards it can be distinguished from the removal of physical inertia and the synthetic inertia introduced by the battery energy storage system after the disturbance. This design choice means that any changes in frequency characteristics can be attributed directly to changes in inertia and not be masked by dispatch adjustments and the inherent variability of renewable energy sources.

The grid-scale BESS placement is an important methodological choice, which directly affects not only the frequency stabilization but also the ability to observe the inertia. The BESS has been connected to bus 16, which was chosen after a careful consideration of the network's architecture, load distribution patterns and the dynamics of disturbance propagation. Bus 16 is electrically close to important transmission interfaces and serves an important load cluster. Frequency disturbances caused by generator failures are especially pronounced at load-dominant buses, especially those located close to inter-area transfer routes. Injecting rapid active power at bus 16 has a significant impact on the frequency nadir and RoCoF, the main characteristics of the system inertia. From the estimation point of view, the BESS is sited at load bus 16, instead of a generator bus, which avoids the artificial enhancement of the frequency response at the disturbance source. This one maintains spatial frequency gradients and adds complexity to the frequency signal used for the inertia estimation.

The BESS is designed to have a system-level impact on system frequency while keeping the system dynamics stable. Its rated power is determined to be equal to 270 MW, which makes up around 4–5% of the overall system load, which is often mentioned in the current research as acceptable for effective frequency support in transmission networks [45,46]. The energy capacity is chosen in the range of 79 MWh and thus allows for sustained power injection in the inertial and initial primary response stages. Inertia emulation only needs to

be supplied with a few seconds of energy, which is a characteristic that avoids premature saturation in optimization adjustments and assures physically plausible performance in repeated simulations. Furthermore, inertia is best excited by disturbances that directly modify the power inertia equilibrium.

The research design includes two structured disturbance scenarios designed in order to evaluate the robustness and accuracy of the suggested hybrid PSO-GA inertia estimation framework under increasing system stress. In Scenario 1, one synchronous generator at bus 38 is tripped at t = 5 s (ensuring that the system is in steady state conditions before the event is triggered), which represents a severe but frequently analyzed contingency within the context of the IEEE 39 bus system. The selection of the generator located at bus 38 is based on the fact that it is a typical synchronous unit and its removal causes both localized frequency variations and inter-area oscillations. Consequently, this configuration exhibits complex dynamic behavior that is very sensitive to changing inertia.

In Scenario 2, a simultaneous generator trip at buses 38 and 32 is introduced at the same disturbance instant, which deliberately reduces the effective synchronous inertia further and increases the magnitude of RoCoF and the frequency nadir. The selection of the generator at bus 32 as the second disturbance was based on an ordered process of inertia impact screening rather than an arbitrary decision. Among the other synchronous units after the first bus 38 trip and PV replacement at bus 37, the generator at bus 32 has a medium- to high-inertia contribution capable of producing a measurable reduction in the equivalent system inertia, but not so great as to force the system into an extreme low-inertia system regime. Tripping this unit thus provides a good analytically tractable decrement in the aggregate inertia constant, allowing meaningful comparison with the single trip case but not sacrificing system stability.

Importantly, the configuration of the BESS and its size do not change between the two scenarios in order to isolate the physical inertia reduction's effect from the artificial compensation changes. This dual-scenario framework allows to systematically compare the estimator behavior, trajectory tracking accuracy and robustness under different disturbance severities validating the hybrid optimization approach under both moderate and more stressed low-inertia operating conditions.

The presence of frequency domain values of an aggregated swing equation is used to approximate system inertia using measured frequency values.

$$f(t) = f(t) - f_0$$

where, f_0 is nominal system frequency.

The unified model is presented in Equation (6):

$$\frac{\partial \Delta f(t)}{\partial t} = \frac{f_0}{2H_{eq}}\left(\Delta P_m(t) - \Delta P_e(t) - D_f \Delta f(t) + \Delta P_{Bess}(t)\right) \tag{6}$$

Equation (6) directly relates the rate of change of the frequency to the net power imbalance with a factor divided by the same of the equivalent system inertia H_{eq}. It summarizes the existing dynamics in the periods of inertial response and primary response that are most predictive to inertia estimate. The value of ΔP_{Loss} and aggregated governor model are modeled as depicted in Equations (7) and (8) respectively.

$$\Delta P_e(t) = \Delta P_Lossu(t - t_f) \tag{7}$$

$$\Delta P_m(s) = \frac{1}{R_{eff}} + \frac{1}{1 + sT_g}(-\Delta f(s)) \tag{8}$$

Lastly, Figure 5 is the block diagram for the test system model, which illustrates the generators, loads, and a BESS connected by the grid. Measurement blocks receive the signal of the generators, and the BESS model of a separate dynamic block is coupled to the grid. The architecture demonstrates how the components of generation, storage and load will be configured and interfaced through the simulation structure.

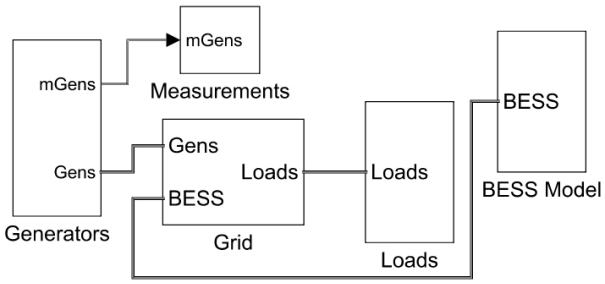


Figure 5. System model block diagram.

2.5. Hybrid PSO-GA Approach

The hybrid PSO-GA algorithm merges the global search of GA with the speed of convergence of PSO and consequently introduces a more successful and stable optimization system of establishing optimal gain settings in complicated control systems [41]. Combining these two metaheuristics into a hybrid algorithm removes the weaknesses inherent in both constituent methods, in particular the propensity of PSO to local optima trapping and the slowness of convergence in GA. As a result, the formulation derived will provide a stronger and more effective strategy for estimating inertia in power systems [47]. This decomposition brings the dimensions of the decision space down, consequently increasing the exploration and exploitation power of the algorithm [48]. Moreover, the hybrid model adds heuristic processes to the stochastic search model to avoid the trapping of local optima as well as to improve the accuracy of the solution, at least in the context of optimal generation supported by improved recommendations [49]. Furthermore, the mixed-method PSO-GA algorithm, which makes use of integer-based encoding of decision variables, is especially capable of solving mixed-integer programming problems that are found in realistic power system optimization, e.g., optimal location and capacity of battery energy storage systems [50]. This general methodology is particularly beneficial to locating solar buses as prospective candidates for deploying battery energy storage where the emulated inertia constant becomes an important decision variable in the optimization task [21].

In general, the proposed hybrid PSO-GA framework presents a sequential cooperative optimization approach, in which PSO is first implemented to conduct a global exploration of the inertial parameter space, and a local refinement is then performed using a GA. An elitist selection mechanism is adopted at each iteration to keep the best performing individuals based on a given fitness criterion, which will improve the robustness of the convergence while reducing the premature stagnation.

The proposed hybrid PSO-GA estimation framework requires to encode the obscure dynamic specifications that organize the response to the frequency of the electrical system, in particular the inertia constant H and, optionally, the dampening coefficient D, primary control gain, K, or the governor time constant T_g. $\left[\theta = \ H, D, K, T_g, \ldots\right]$.

As illustrated in Figure 6, the approach starts with the initialization of PSOGA variables, i.e., the population of particles and their velocities are generated in permissible physical limits of $\theta_{min} \leq \theta \leq \ \theta_{max}$. With the reduced order swing model, the resulting

simulated frequency course for a disturbance with a known active power imbalance $\Delta P(t)$ is generated, as depicted in Equation (9).

$$2H\frac{d\omega}{dt} = \Delta P(t) - D(\omega - \omega_0) - K(\omega - \omega_0) \tag{9}$$

where H is the inertia constant of the equivalent system, while ω and ω_0 represent the rotor angular speed and the nominal (synchronous) angular speed respectively. The term $\frac{d\omega}{dt}$ describes the rate of change of rotor speed, capturing the system's inertial response to disturbances. The quantity $\Delta P(t)$ is the time-varying power imbalance between mechanical input and electrical output. The damping coefficient D accounts for speed-dependent damping effects, whereas K represents an additional frequency-responsive control or stiffness gain, such that the terms $D(\omega - \omega_0)$ and $K(\omega - \omega_0)$ collectively model the dissipation and corrective control actions acting against deviations from the nominal speed.

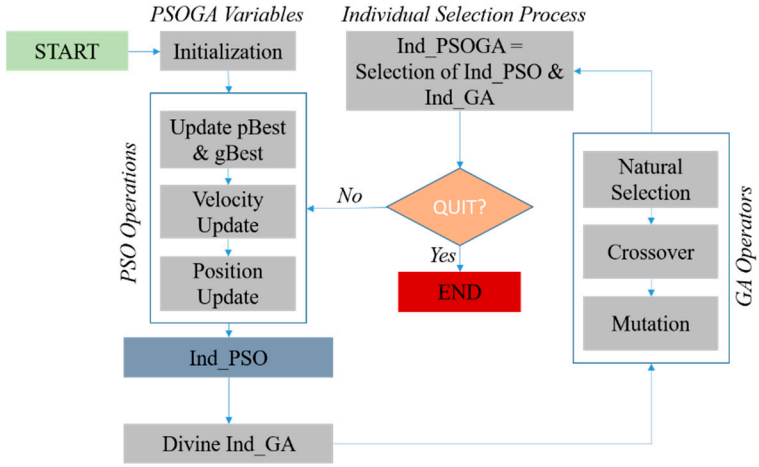


Figure 6. PSO-GA algorithm flowchart.

The objective function shown in Equation (10) decreases with the help of the hybrid search mechanism measurements, assessing both the simulated and measured frequency time series, like RoCOF, in a given time window, the length of which is called T. This relation can be expressed mathematically as follows:

$$J(\theta) = \sum_{t \in T} \omega f(\omega_{meas}(t) - \omega_{sim}(t;\theta))^2 + \omega_r\left(\dot{\omega}_{meas}(t) - \dot{\omega}_{sim}(t;\theta)\right)^2 + \lambda\|\theta - \theta_0\|_2^2 \tag{10}$$

The cost function, J, of the ROCOF calculation, along with the small Tikhonov regularization term, λ, which biases the estimate with the desired initial condition $J(\theta_i)$ towards higher values resulting in smaller cost values, is found to optimize the performance of the PSO algorithms on estimating parameters. These algorithms have the particle that compares $J(\theta_i)$ and, later, optimizes their personal best ($pBest_i$) and the optimum of the global best ($gBest$). After this, positions and velocities are updated through Equation (11).

$$v_i^{k+1} = \omega_I v_i^k + c_1 r_1\left(pBest_i - \theta_i^k\right) + c_2 r_2\left(gBest_i - \theta_i^k\right), \qquad \theta_i^{k+1} = \theta_i^k + v_i^{k+1} \tag{11}$$

where ω_I is the inertia weight, c_1 and c_2 are coefficients of cognitive acceleration and r_1 and r_2 are randomly chosen points of the range (0, 1). Likewise, $v_i^{(k+1)}$ denotes the velocity of the ith particle at iteration $k+1$, while v_i^k is its velocity at the previous iteration. Simultaneously, the GA element supports natural selection to the existing population using the past and future where the frequency data are contaminated by noise or the mapping smoke $\theta \mapsto \omega_{sim}$ is challenging to determine; the aspect of the algorithm is

highly significant in these cases. The individual selection process then combines the PSO trace-expanded set Ind_{PSO} with the GA-generated set Ind_{GA} through an elitist replacement process that replaces the worst offenders of the set with the best offenders of the set; at the same time, the parameter constraints are enforced, resulting in a new generation pool Ind_{PSOGA}.

The loop is stopped when one of the following stopping conditions is satisfied: $k \geq k_{max}$, $\|J^k - J^{k-1}\| < \epsilon$, *or* $\|gBest^k - gBest^{k-1}\| < \delta$. Afterwards the algorithm produces the final population, which is expressed as $\hat{\theta} = gBest$, named Ind_{GA}/END, where the inertia estimate, $\hat{H}$, is calculated. A combination of high velocity convergence of PSO to optimal areas $gBest$ and the exploring nature of GA, the PSO-GA model provides an efficient optimization-driven estimator of system inertia. This estimation maintains precision in the noisy measurement cases and resilience to multiple model error landscapes, as well as has computational efficiency that is appropriate to real-time or post-event inertia measurement in low-inertia power grids.

3. Results

The proposed inertia estimation technique has been implemented on a scenario-based test system with IEEE 39 bus, RES and BESS being incorporated on a grid scale to evaluate the dynamic behavior of three optimization algorithms—Hybrid PSO-GA, PSO, and GA—in determining the equivalent inertia constant of the system. The optimization procedures and subsequent performance analyses are carried out in Python, enabling efficient algorithm implementation, statistical evaluation, and comparative assessment of the proposed methods. To simulate a real-life frequency disturbance, a generation trip disturbance was provided at $t = 5$ s. The actual total inertia of the two scenarios was calculated at 4.5 s and 4.11 s, which is a typical weight for a mid-range size interconnected grid. The BESS was set up to enable synthetic inertia as well as quick frequency support through active power injection in the case of post-disturbance transients.

As depicted in Figure 7 (scenario 1), following a disturbance, the system frequency falls from 50.00 Hz down to a low of about 49.76 Hz, which then returns to normal in about 4.49 s. Figure 7 shows the frequency variations as measured in the real system compared with the frequency variations predicted by the use of, for the inertia, the three different methods. The curve from HPSO is similar to the measured frequency: the lowest point is at approximately 49.74 Hz (0.03 Hz more than the actual minimum) and the recovery process is similar. The PSO approach produces a more pronounced frequency drop to 49.70 Hz followed by a more gradual recovery to 50 Hz, whereas the GA approach delivers 49.67 Hz with the longest settling time. These differences indicate that the HPSO method is a better representation of the dynamic characteristics of the system. In contrast, both the PSO and GA methods seem to overpredict the inertia and hence produce underdamped or delayed frequency responses.

Conversely, when two synchronous generators at bus 38 and bus 32 are tripped at the same time at t = 5 s, as shown in Figure 8, the frequency response demonstrates a stronger transient than in Scenario 1 because of the loss of generation, as well as because of the reduced effective inertia. As demonstrated in Figure 8, the system frequency decreases from 50.00 Hz to about 49.56 Hz before the start of recovery. The HPSO method tracks the measured curve closely, reaching the bottom of the depth of 49.58 Hz, which is almost exactly the same as the observed one (a difference of only approximately 0.02 Hz), as well as the recovery time of 4.11 s that is virtually the same as that observed. However, the standalone PSO predicts an even less accurate response, with a minimum of about 49.60 Hz, whereas the GA method has the highest deviation with a value of about 49.57 Hz and a settling time of 4.23 s. Moreover, RoCof proves the fact that Scenario 2 creates a steeper

initial slope magnitude compared with Scenario 1, which is also in line with the lower effective inertia and the higher disturbance magnitude. The HPSO-based trajectory best captures the magnitude of peak RoCoF as well as the damping behavior of the oscillatory tail, but PSO and GA have slight differences in the transient curvature and the recovery rate. These discrepancies suggest that the hybrid PSO-GA model represents the enhanced nonlinear behavior caused by the dual-generator outage better than standalone PSO and GA, and the inertia and damping interaction is slightly underrepresented in capabilities of the small but significant deviations in the nadir depth and recovery properties.

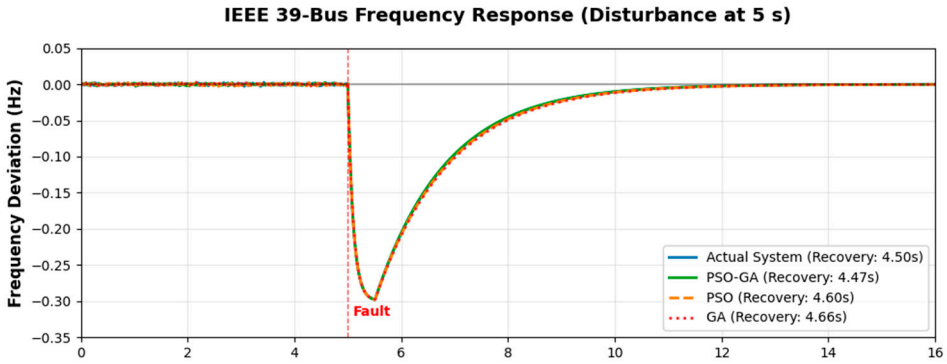


Figure 7. Scenario 1. Frequency response comparison (real vs estimated using HPSO, PSO, and GA).

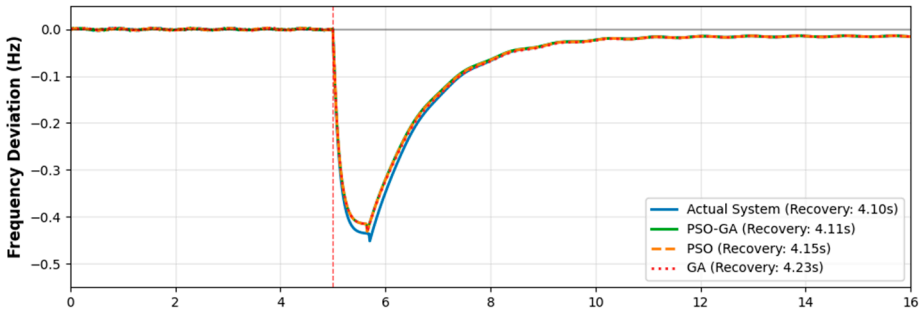


Figure 8. Scenario 2. Frequency response comparison (real vs estimated using HPSO, PSO, and GA).

In Scenario 1 (single generator trip at bus 38), HPSO achieves a root mean square error (RMSE) of 0.011 Hz and a mean absolute percentage error (MAPE) of 0.022%, demonstrating a substantial improvement over the standalone optimization methods. In comparison, the conventional PSO results in an RMSE of 0.027 Hz and a MAPE of 0.055%, while the GA yields higher errors with an RMSE of 0.041 Hz and a MAPE of 0.083%. In terms of inertia estimation accuracy, HPSO predicts an inertia constant of 4.49 s, which closely matches the actual system inertia of 4.5 s. By contrast, PSO and GA overestimate the inertia constant, producing values of 4.62 s and 4.67 s, respectively. The values in the result support the idea that, although all the algorithms meet in the moderate circumstances of disturbance, the hybrid approach significantly reduces frequency domain trajectory error as well as parameter estimation bias. The very low value of the RMSE and the very small mean absolute percentage error (MAPE) observed in Scenario 1 suggest a well-conditioned optimization landscape, with high inertia identifiability and small nonlinear interactions.

The case of Scenario 2, when the contingencies occurred at bus 38 and bus 32 at the same time, the effective inertia decreases to 4.10 s, which further emphasizes the electromechanical transient and increased RoCoF. Table 3 shows that this situation results in more significant estimation errors in all the methods. The hybrid PSO-GA algorithm estimates 4.11 s with RMSE = 0.015 Hz and MAPE = 0.73%, PSO only estimates 4.18 s (RMSE = 0.0246 Hz,

MAPE = 1.95%), and GA estimates 4.23 s (RMSE = 0.0289 Hz, MAPE = 3.17%). In spite of the absolute RMSE and MAPE values getting worse compared with Scenario 1—greater dynamic nonlinearity and steeper curvature of the cost function—the relative ranking of the algorithms does not change. The hybrid technique has minimum variation in the actual inertia and the lowest trajectory error, therefore proving to be resilient to compound disturbances. The significant increase in MAPE of GA by 0.083 to 3.17 and that of PSO by 0.055 to 1.95 makes it clear that the two systems are more sensitive to lower inertia and a greater coupling between the inertia, damping, and system dynamics. On the other hand, the insignificant variation in RMSE of the hybrid PSO-GA (0.011 to 0.015 Hz) verifies that the composite structure maintains the stability of convergence even when the stress of the system is intensified.

Table 3. Comparison of inertia estimation performance under single and dual generator trip scenarios.

	Algorithm	Estimated Inertia	RMSE (Hz)	MAPE (%)
Scenario 1 (Bus 38 Generator Trip)	Hybrid PSO-GA	4.49	0.011	0.022
	PSO	4.62	0.027	0.055
	GA	4.67	0.041	0.083
Scenario 2 (Bus 38 + 32 Generator Trips)	Hybrid PSO-GA	4.11	0.015	0.73
	PSO	4.18	0.0246	1.95
	GA	4.23	0.0289	3.17

Even when the disturbance level increases, the estimation difficulties intensify and the error rates are higher; the hybrid PSO-GA system is always more accurate and robust than the presented PSO and GA algorithms. The low RMSE and low inertia deviation factor are sustained in the 4.50 and 4.10 s operating regimes in support of the appropriateness of the algorithm in low-inertia power systems operating under harsh contingencies.

Over all, these results confirm that the proposed HPSO framework provides superior estimation accuracy and robustness, particularly in the presence of BESS-induced fast frequency dynamics and low-inertia power systems These findings are summarized in Table 3.

Furthermore, the convergence trajectories of PSO-GA exhibit reduced oscillations around the optimal solution, indicating improved robustness against premature convergence. The contribution of the BESS to frequency stability is evaluated by comparing the system responses under operating conditions with and without energy storage. In the absence of BESS support in the first scenario, the system frequency declines to approximately 49.70 Hz, followed by a slow recovery governed solely by conventional regulation mechanisms. As shown in Figure 9, when the BESS is integrated, the frequency nadir improvesto 49.86 Hz, and the recovery time to the nominal frequency of 50 Hz is significantly reduced. Specifically, the frequency recovery time decreases from 10.2 s without BESS to 2.6 s with BESS, corresponding to a reduction of approximately 40%. During the initial seconds following the disturbance, the BESS contributes synthetic inertia in the range of approximately 1.0–1.8 s, supplying temporary active power support that effectively limits the frequency decline and accelerates the subsequent recovery.

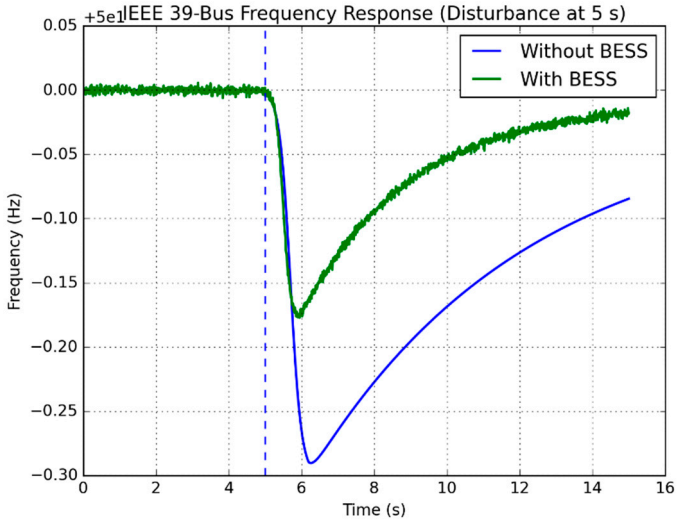


Figure 9. Scenario 1. Frequency response of the IEEE 39 bus system with and without BESS support of a fault at t = 5 s. With BESS, the frequency nadir is shallower (49.86 Hz) and recovery is faster compared with the system operating without storage (49.70 Hz).

One of the roles of the BESS is to support a rapid pulse of dispatchable power (around 8% of named capacity) just after a disturbance initially occurs, then a rapid decay as the system frequency returns to normal. The equivalent inertia contribution shows a significant rise in the first second after the disturbance, its maximum is reached at about 1.8 s, and then falls off as the power injection dissipates.

Figure 10 shows that by tripping two generators (695 MW) simultaneously, the magnitude of the disturbance increases and the effective physical inertia reduces, further enhancing the RoCoF and increasing the frequency excursion in the absence of BESS. The loss of two generators compounding the first slope of the frequency decadence and increasing the recovery rate highlights the fact that the inertia, damping, and governor action are nonlinearly coupled with each other. Since the BESS setup is already held at the same level as Scenario 1, its stabilizing influence is even greater in the compounded disturbance case. The storage system suppresses the extra power imbalance by injecting rapid synthetic power, which in effect moderates the RoCoF and limits the nadir, although the inertia of synchronous is reduced. Even though the absolute deviations of Scenario 2 are bigger than those of Scenario 1 (see Figure 10), the qualitative gain of the BESS is similar to it: a smaller peak deviation, faster arrest of the frequency decay, shorter exponential recovery, and observable higher damping of oscillatory content. In general, the comparative outcomes in the two cases prove that the intensification of disturbance decreases natural inertia and increases frequency indicators in the condition of the absence of support, whereas the introduction of a grid-scale BESS leads to a significant improvement in transient stability, reduction in the amplification of RoCoF and enforced recovery in low-inertia operating regimes.

The improved performance of the proposed hybrid PSO-GA approach arises from its hybrid search mechanism, which effectively combines the global exploration capability of GA with the rapid local convergence characteristics of particle swarm optimization, as depicted in Figures 11a and 12a. This complementary interaction enables HPSO to efficiently navigate the nonlinear optimization landscape associated with inertia estimation, resulting in enhanced numerical stability and convergence toward an inertia value that closely matches the actual system parameter.

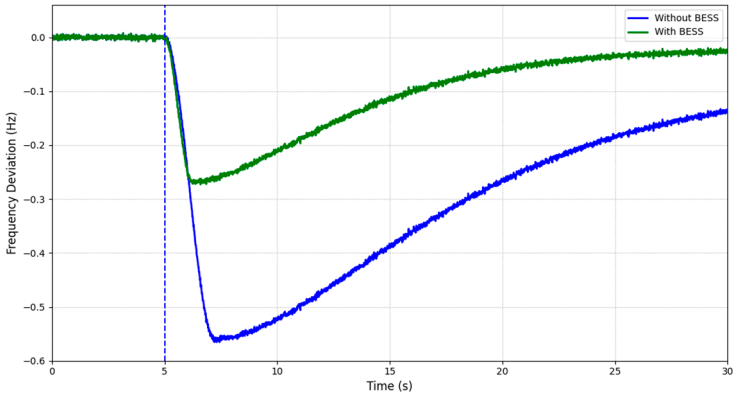


Figure 10. Scenario 2. Frequency response of the IEEE 39 bus system with and without BESS support of a fault at t = 5 s. With BESS, the frequency nadir is shallower (49.73 Hz) and recovery is faster compared with the system operating without storage (49.42 Hz).

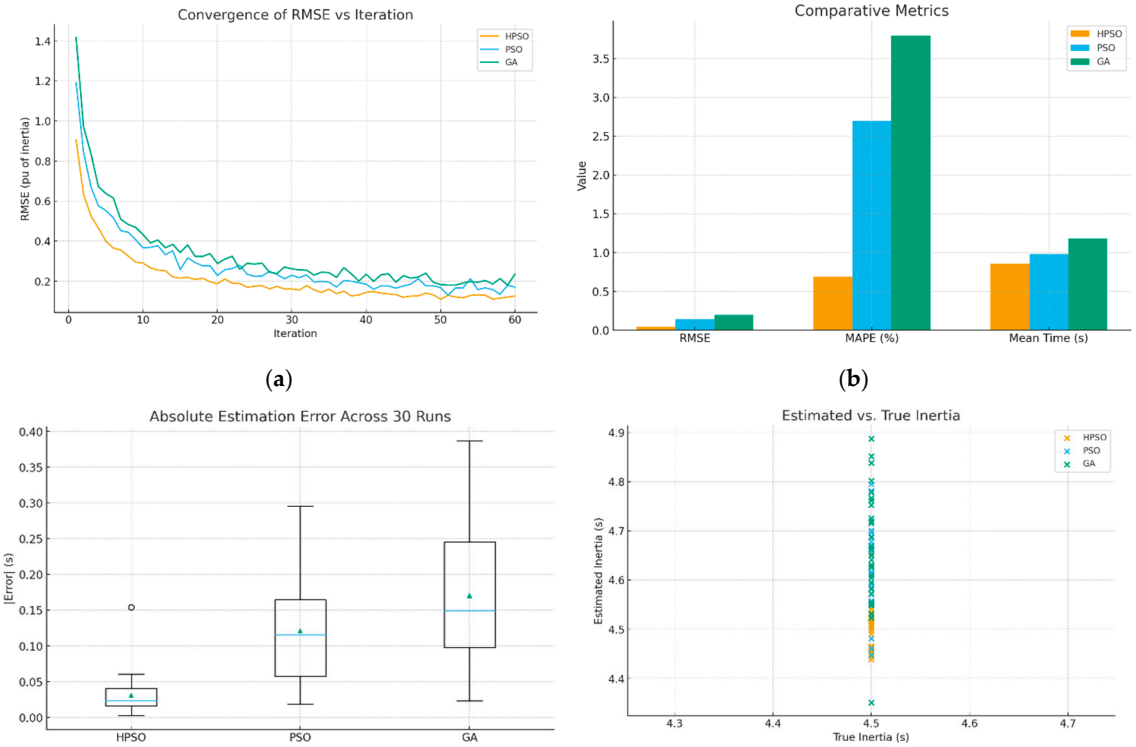


Figure 11. Scenario 1. (**a**) RMSE convergence vs no. of iterations; (**b**) error comparison; (**c**) absolute estimation error box plot for I = 30; (**d**) scatter of the estimated vs true inertia.

The HPSO approach has the best equilibrium between estimation precision, dynamical reactivity and computational efficiency. Comparatively, as depicted in Figures 11c and 12c, the hybrid PSO-GA saves the computation time of PSO or GA, and the estimation error is almost 4 times smaller across the iterations. The reconstructed frequency trajectories show good agreement with the actual system response compared with PSO and GA, which show delayed recovery and diverge in the steady state. These results validate that HPSO is a practical and accurate method for practical inertia estimation in power systems, with a significant degree of converter-interfaced resource integration, as shown in both Figures 11d and 12d. Through the addition of both physical and synthetic inertia effects, it can be used for the adaptive frequency regulation and stability evaluation of future low-inertia power grids. The capability of the method to model and track equivalent inertia

provided by dynamically acting BESS equipment makes it an identity square for grid operators trying to assess and manage frequency toughness within fluctuating circumstances.

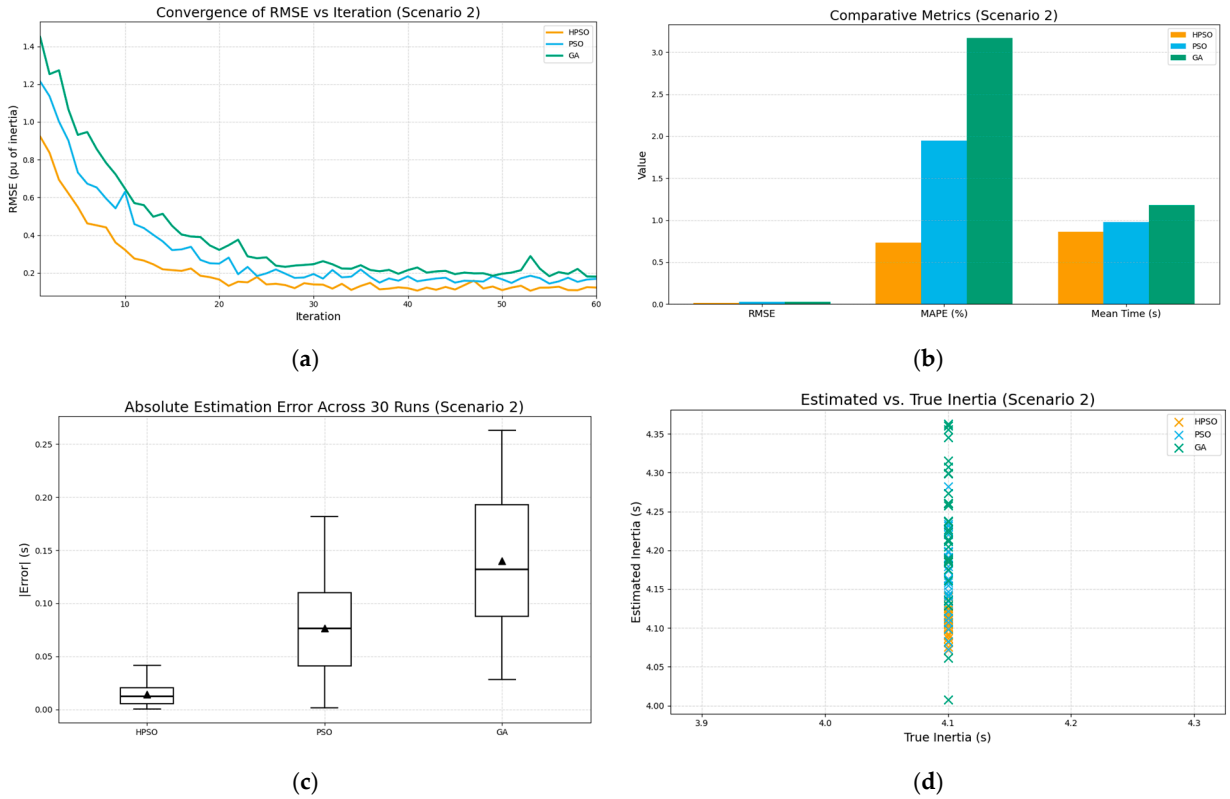


Figure 12. Scenario 2. (**a**) RMSE convergence vs no. of iterations; (**b**) error comparison; (**c**) absolute estimation error box plot for I = 30; (**d**) scatter of the estimated vs true inertia.

A clear trend is observed when comparing the two situations. In Scenario 1 (single generator trip at bus 38), all algorithms run in a relatively nonlinear regime, and the hybrid PSO-GA has already provided the best accuracy (4.49 s compared with the real value of 4.5 s) with the lowest root mean square error (RMSE) and mean absolute percentage error (MAPE), as presented in Table 3, Figures 11b and 12b. The estimation problem in Scenario 2 is more complicated by the presence of compounded electromechanical interactions and increased coupling between terms of inertia, damping, and governors. Despite the fact that absolute estimation errors have grown in all the methods, the relative performance rankings are left unchanged: HPSO has less inertia deviation and the most stable convergence of RMSE behavior throughout iterations, with PSO having moderate overestimation and the biggest dispersion in the genetic algorithm (GA). Notably, the BESS setup is purposely maintained the same in both cases and, as such, variation in the estimation performance could be entirely attributable to the severity of disturbances and not to the adjusted synthetic inertia parameters. Such consistency confirms that the hybrid estimator is sturdy to changes in the magnitude of disturbances and also that it is reliable in tracking the same inertia when the system stress is increased.

Although the numerical improvement of the hybrid PSO–GA over standalone PSO and GA may appear moderate in absolute RMSE terms, its significance should be interpreted in the context of inertia parameter sensitivity. In low-inertia power systems, even small deviations in the estimated equivalent inertia constant can lead to noticeable discrepancies in predicted RoCoF, frequency nadir, and transient stability margins. The hybrid method not only achieves the lowest steady-state RMSE but also demonstrates smoother and more stable convergence behavior, as illustrated in Figures 11a and 12a. This reduced oscillatory

behavior and improved monotonic convergence enhance robustness and repeatability of the estimation process. Therefore, the improvement is practically meaningful in dynamic frequency analysis and operational inertia awareness, where estimation reliability and stability are as critical as absolute numerical accuracy.

4. Conclusions

This research introduces a novel hybrid framework combining PSO and GA for the accurate and adaptable estimation of the inertia of the power systems with grid-scale BESS. The hybrid approach evaluated in two scenarios based on the IEEE 39 bus test system shows better performance compared with the traditional methods of PSO and GA in terms of estimation accuracy and calculation efficiency. The HPSO approach can combine the global search ability of the GA and the fast convergence ability of the PSO, which results in a better solution quality and higher robustness. The results of the simulation in Scenario 1 showed that the value of inertia by HPSO (4.49 s) was very close to the actual system inertia (4.5 s) and the smallest RMSE (0.011 Hz) and MAPE (0.022%) were obtained from all of the methods. Similarly, in Scenario 2, where the system is in intensified low-inertia stress conditions, the hybrid PSO–GA achieved an estimated inertia of 4.11 s against the true 4.10 s, with RMSE = 0.0152 Hz and MAPE = 0.73%, outperforming standalone PSO (RMSE = 0.0246 Hz, MAPE = 1.95%) and GA (RMSE = 0.0289 Hz, MAPE = 3.17%).

On the other hand, PSO and GA resulted in larger estimation errors and less rapid dynamic response. Furthermore, the trajectories of frequencies estimated by HPSO closely resembled the observed response of the system, hence confirming the superior accuracy of the hybrid approach.

The introduction of BESS proved to improve the level of frequency stability that was provided by them through the supply of a "synthetic inertia", in this case where the frequency nadir had to be lowered from 49.70 Hz to 49.86 Hz in Scenario1 and 49.42 Hz to 49.73 Hz in Scenario 2 and that the recovery time was shortened by around 40%. The proposed estimator was able to accurately estimate the dynamic equivalent inertia contributed by the BESS, which was found to vary from 1.0 s to 1.8 s during post-disturbance transients in Scenario 1. These results prove that HPSO can be successfully used for effectively monitoring time-varying inertia in the nonlinear and converter-dominated grid environments.

Although estimation errors increased in Scenario 2 relative to Scenario 1 due to stronger nonlinearity and steeper transient behavior, the convergence analysis demonstrated that HPSO maintained better accuracy. Overall, Scenario 2 confirms that, while compounded generator outages amplify frequency excursions and increase optimization complexity, the proposed hybrid PSO–GA framework preserves high estimation accuracy and strong robustness under severe low-inertia conditions with fixed BESS support.

Overall, the results show empirical convergence evidence of the proposed hybrid PSO–GA framework, characterized by rapid RMSE reduction in early iterations and stable plateau behavior at later stages. The elitist replacement mechanism ensures monotonic non-increasing best-so-far fitness values, contributing to practical convergence robustness. While formal convergence proofs for hybrid stochastic metaheuristics in nonlinear multimodal power-system identification problems are analytically intractable, the observed empirical stabilization and superior RMSE performance validate the effectiveness of the proposed approach.

In contrast with previous methodologies based only on the offline parameter identification, the HPSO-based approach proposes a more robust mechanism for the real-time parameter estimation, suitable to integrate into wide area monitoring and control systems. Its reliable convergence properties make it particularly suitable for online application in power systems that process usability to inertia fluctuations occurring due to the variability

of renewable energy and the rapid interventions made on storage. These results are in line with the recent research that highlights the importance of data-driven and hybrid methods for dynamic model parameter estimation.

Future research will focus on the extension of this framework to systems with multi-areas, real-time digital simulation and high RES integration. This will help establish its efficacy in actual real-world scenarios with communication time delays and measurement errors. Moreover, the use of the HPSO estimator in conjunction with machine learning forecasting models could be used to enhance the accuracy of inertia predictions in systems with a lot of renewable energy.

Author Contributions: Conceptualization, M.F.A. and Y.Y.; methodology, M.F.A.; software, M.F.A.; validation, M.F.A. and Y.Y.; writing—original draft preparation, M.F.A.; writing—review and editing, M.F.A. and Y.Y.; supervision, Y.Y. All authors have read and agreed to the published version of the manuscript.

Funding: This research received no external funding.

Data Availability Statement: The data presented in this study are available on request from the corresponding author.

Acknowledgments: During the preparation of this manuscript, the authors hereby acknowledge the use of AI-assisted tools, specifically Grammarly and ChatGPT to enhance linguistic clarity and correct grammatical inconsistencies. All content generated with the assistance of these tools was carefully reviewed and edited by the authors, who take full responsibility for the integrity and originality of the published work. The use of AI-assisted tools complies with the journal's policies on transparency and ethical standards in authorship.

Conflicts of Interest: The authors declare no conflicts of interest.

Abbreviations

The following abbreviations are used in this manuscript:

RoCoF	Rate of Change of Frequency
PSO	Particle Swarm Optimization
GA	Genetic Optimization
PSO-GA	Particle Swarm Optimization–Genetic Optimization
BESS	Battery Energy Storage Systems
RES	Renewable Energy Source
HPSO	Hybrid Particle Swarm Optimization (PSO-GA)

References

1. Wu, B.; Yu, X.; Brika, S.K.; Sultan, M.S.; Liu, H. Balancing household energy efficiency supply and demand: The role of energy storage in integrating renewable energy sources. *Energy Build.* **2025**, *347*, 116253. [CrossRef]
2. Tan, B.; Zhao, J.; Netto, M.; Krishnan, V.; Terzija, V.; Zhang, Y. Power system inertia estimation: Review of methods and the impacts of converter-interfaced generations. *Int. J. Electr. Power Energy Syst.* **2022**, *134*, 107362. [CrossRef]
3. Deng, X.; Mo, R.; Wang, P.; Chen, J.; Nan, D.; Liu, M. Review of RoCoF Estimation Techniques for Low-Inertia Power Systems. *Energies* **2023**, *16*, 3708. [CrossRef]
4. Zografos, D. *Power System Inertia Estimation and Frequency Response Assessment*; KTH Royal Institute of Technology: Stockholm, Sweden, 2019.
5. Jain, S.K. A Review on Power System Inertia Estimation Techniques. In *2021 International Conference on Control, Automation, Power and Signal Processing (CAPS)*; IEEE: New York, NY, USA, 2021; pp. 1–6. [CrossRef]
6. Abouyehia, M.; Egea-Àlvarez, A.; Ahmed, K.H. Evaluating inertia estimation methods in low-inertia power systems: A comprehensive review with analytic hierarchy process-based ranking. *Renew. Sustain. Energy Rev.* **2025**, *217*, 115794. [CrossRef]
7. Dimoulias, S.C.; Kontis, E.O.; Papagiannis, G.K. Inertia Estimation of Synchronous Devices: Review of Available Techniques and Comparative Assessment of Conventional Measurement-Based Approaches. *Energies* **2022**, *15*, 7767. Available online: https://EconPapers.repec.org/RePEc:gam:jeners:v:15:y:2022:i:20:p:7767-:d:948652 (accessed on 10 December 2025). [CrossRef]

8. Mehrzad, A.; Darmiani, M.; Rouhani, S.H.; Su, C.L.; Sepestanaki, M.A.; Mofidipour, E.; Monti, A.; Anvari-Moghaddam, A. Inertia in renewable power systems: A review of estimation methods and practical implementation. *Renew. Sustain. Energy Rev.* **2026**, *226*, 116246. [CrossRef]
9. Heylen, E.; Teng, F.; Strbac, G. Challenges and opportunities of inertia estimation and forecasting in low-inertia power systems. *Renew. Sustain. Energy Rev.* **2021**, *147*, 111176. [CrossRef]
10. Prabhakar, K.; Jain, S.K.; Padhy, P.K. Inertia estimation in modern power system: A comprehensive review. *Electr. Power Syst. Res.* **2022**, *211*, 108222. [CrossRef]
11. Peng, J.; Tan, J.; Koralewicz, P.; Mendiola, E.; Dong, S.; Hoke, A.; Horowitz, K. Probing Signal-Based Inertia and Frequency Response Estimation for Power Systems With High Levels of Inverter-Based Resources. In *2024 IEEE Power & Energy Society General Meeting (PESGM)*; IEEE: New York, NY, USA, 2024; pp. 1–5. [CrossRef]
12. Zografos, D.; Ghandhari, M. Power system inertia estimation by approaching load power change after a disturbance. In *2017 IEEE Power & Energy Society General Meeting*; IEEE: New York, NY, USA, 2017; pp. 1–5. [CrossRef]
13. Ashton, P.M.; Saunders, C.S.; Taylor, G.A.; Carter, A.M.; Bradley, M.E. Inertia Estimation of the GB Power System Using Synchrophasor Measurements. *IEEE Trans. Power Syst.* **2015**, *30*, 701–709. [CrossRef]
14. Chassin, D.P.; Huang, Z.; Donnelly, M.K.; Hassler, C.; Ramirez, E.; Ray, C. Estimation of WECC System Inertia Using Observed Frequency Transients. *IEEE Trans. Power Syst.* **2005**, *20*, 1190–1192. [CrossRef]
15. Tan, B.; Zhao, J. Data-Driven Adaptive Unscented Kalman Filter for Time-Varying Inertia and Damping Estimation of Utility-Scale IBRs Considering Current Limiter. *IEEE Trans. Power Syst.* **2024**, *39*, 7331–7345. [CrossRef]
16. Del Giudice, D.; Grillo, S. Analysis of the Sensitivity of Extended Kalman Filter-Based Inertia Estimation Method to the Assumed Time of Disturbance. *Energies* **2019**, *12*, 483. [CrossRef]
17. Lugnani, L.; Dotta, D.; Lackner, C.; Chow, J. ARMAX-based method for inertial constant estimation of generation units using synchrophasors. *Electr. Power Syst. Res.* **2020**, *180*, 106097. [CrossRef]
18. Yin, H.; Wu, Y.; Qiu, W.; Zeng, C.; You, S.; Tan, J.; Hoke, A.; Kruse, C.J.; Rockwell, B.W.; Kawamura, K.A.; et al. Precise ROCOF estimation algorithm for low inertia power grids. *Electr. Power Syst. Res.* **2022**, *209*, 107968. [CrossRef]
19. You, S.; Li, H.; Liu, S.; Sun, K.; Wang, W.; Qiu, W.; Liu, Y. Calculate Center-of-Inertia Frequency and System RoCoF Using PMU Data. In *2021 IEEE Power & Energy Society General Meeting (PESGM)*; IEEE: New York, NY, USA, 2020; pp. 1–5. Available online: https://api.semanticscholar.org/CorpusID:225062326 (accessed on 10 December 2025).
20. Paidi, E.S.N.R.; Marzooghi, H.; Yu, J.; Terzija, V. Development and Validation of Artificial Neural Network-Based Tools for Forecasting of Power System Inertia With Wind Farms Penetration. *IEEE Syst. J.* **2020**, *14*, 4978–4989. [CrossRef]
21. Muhammed, A.O.; Isbeih, Y.J.; Moursi, M.S.E.; Elbassioni, K. Artificial Intelligence (AI) Advanced Techniques for Real-Time Inertia Estimation in Renewable-Based Power Systems. *IEEE Trans. Ind. Appl.* **2025**, *61*, 2604–2619. [CrossRef]
22. Tuo, M.; Li, X. Machine Learning Assisted Inertia Estimation Using Ambient Measurements. *IEEE Trans. Ind. Appl.* **2023**, *59*, 4893–4903. [CrossRef]
23. Hosaka, N.; Berry, B.; Miyazaki, S. The World's First Small Power Modulation Injection Approach for Inertia Estimation and Demonstration in the Island Grid. In *2019 8th International Conference on Renewable Energy Research and Applications (ICRERA)*; IEEE: New York, NY, USA, 2019; pp. 722–726. [CrossRef]
24. Zografos, D.; Ghandhari, M.; Paridari, K. Estimation of power system inertia using particle swarm optimization. In *2017 19th International Conference on Intelligent System Application to Power Systems (ISAP)*; IEEE: New York, NY, USA, 2017; pp. 1–6. [CrossRef]
25. Pang, Y.; Li, F.; Qian, H.; Liu, X.; Yao, Y. A Snake Optimization Algorithm-Based Power System Inertia Estimation Method Considering the Effects of Transient Frequency and Voltage Changes. *Energies* **2024**, *17*, 4430. [CrossRef]
26. Lavanya, L.; Swarup, K.S. Continuous Real-Time Estimation of Power System Inertia Using Energy Variations and Q-Learning. *IEEE Open J. Instrum. Meas.* **2023**, *2*, 9000111. [CrossRef]
27. Tuo, M.; Li, X. Long-Term Recurrent Convolutional Network-based Inertia Estimation using Ambient Measurements. In Proceedings of the 2022 IEEE Industry Applications Society Annual Meeting (IAS), Detroit, MI, USA, 9–14 October 2022. [CrossRef]
28. Pombo, D.V.; Iov, F. Frequency Provision with Low-Inertia Hybrid Power Plants: Identifying Gaps in the Standards. In *4th International Hybrid Power Systems Workshop Energynautics*; AAU Energy: Aalborg, Denmark, 2019.
29. Pati, S.S.; Subudhi, U.; Mishra, S. Robust Frequency Regulation Management System in a Renewable Hybrid Energy Network with Integrated Storage Solutions. *Electricity* **2025**, *6*, 22. [CrossRef]
30. Fernández-Guillamón, A.; Gómez-Lázaro, E.; Muljadi, E.; Molina-García, Á. Power systems with high renewable energy sources: A review of inertia and frequency control strategies over time. *Renew. Sustain. Energy Rev.* **2019**, *115*, 109369. [CrossRef]
31. Tuttelberg, K.; Kilter, J.; Wilson, D.; Uhlen, K. Estimation of Power System Inertia From Ambient Wide Area Measurements. *IEEE Trans. Power Syst.* **2018**, *33*, 7249–7257. [CrossRef]

32. Chang, J.; Du, Y.; Chen, X.; Lim, E.; Wen, H.; Li, X.; Jiang, L. Frequency regulation in adaptive virtual inertia and power reserve control with high PV penetration by probabilistic forecasting. *Front. Energy Res.* **2022**, *10*, 929113. [CrossRef]
33. Rezkalla, M.M.N. *Emulated Inertia and Frequency Support from Fast Acting Reserves Comparative Assessment and Experimental Validation*; Danmarks Tekniske Universitet: Copenhagen, Denmark, 2018.
34. Moraes, G.R.; Ilea, V.; Berizzi, A.; Pisani, C.; Giannuzzi, G.; Zaottini, R. A Perturbation-Based Methodology to Estimate the Equivalent Inertia of an Area Monitored by PMUs. *Energies* **2021**, *14*, 8477. [CrossRef]
35. Zhang, N.; Yan, J.; Hu, C.; Sun, Q.; Yang, L.; Gao, D.W.; Guerrero, J.M.; Li, Y. Price-Matching-Based Regional Energy Market With Hierarchical Reinforcement Learning Algorithm. *IEEE Trans. Ind. Inform.* **2024**, *20*, 11103–11114. [CrossRef]
36. Shaikh, M.S.; Lin, H.; Xie, S.; Dong, X.; Lin, Y.; Shiva, C.K.; Mbasso, W.F. An intelligent hybrid grey wolf-particle swarm optimizer for optimization in complex engineering design problem. *Sci. Rep.* **2025**, *15*, 18313. [CrossRef]
37. Shaikh, M.S.; Raj, S.; Babu, R.; Kumar, S.; Sagrolikar, K. A hybrid moth–flame algorithm with particle swarm optimization with application in power transmission and distribution. *Decis. Anal. J.* **2023**, *6*, 100182. [CrossRef]
38. Hu, P.; Li, Y.; Yu, Y.; Blaabjerg, F. Inertia estimation of renewable-energy-dominated power system. *Renew. Sustain. Energy Rev.* **2023**, *183*, 113481. [CrossRef]
39. Pallero, J.L.G.; Fernández-Martínez, J.L.; Fernández-Muñiz, Z.; Bonvalot, S.; Gabalda, G.; Nalpas, T. GravPSO2D: A Matlab package for 2D gravity inversion in sedimentary basins using the Particle Swarm Optimization algorithm. *Comput. Geosci.* **2021**, *146*, 104653. [CrossRef]
40. Zaki, M.; Shahin, A.; Eskender, S.; Elsayes, M.A. Improving efficiency of parallel inverters operation in island mode microgrids. *Sci. Rep.* **2023**, *13*, 20738. [CrossRef]
41. Bansal, R.C. Optimization Methods for Electric Power Systems: An Overview. *Int. J. Emerg. Electr. Power Syst.* **2005**, *2*, 1. [CrossRef]
42. Pavon, W.; Jaramillo, M.; Vasquez, J.C. A Review of Modern Computational Techniques and Their Role in Power System Stability and Control. *Energies* **2023**, *17*, 177. [CrossRef]
43. Ge, L.; Liu, J.; Wang, B.; Zhou, Y.; Yan, J.; Wang, M. Improved adaptive gray wolf genetic algorithm for photovoltaic intelligent edge terminal optimal configuration. *Comput. Electr. Eng.* **2021**, *95*, 107394. [CrossRef]
44. Soares, J.; Valle, Z.; Morais, H. Decision support tool for Virtual Power Players: Hybrid Particle Swarm Optimization applied to Day-ahead Vehicle-To-Grid Scheduling. In *7th International Conference on Intelligent System Applications to Power Systems (ISAP 2013)*; IEEE: New York, NY, USA, 2013. Available online: https://orbit.dtu.dk/en/publications/decision-support-tool-for-virtual-power-players-hybrid-particle-s/ (accessed on 4 January 2026).
45. Ghoshal, S.P. Optimizations of PID gains by particle swarm optimizations in fuzzy based automatic generation control. *Electr. Power Syst. Res.* **2004**, *72*, 203–212. [CrossRef]
46. Golpîra, H.; Atarodi, A.; Amini, S.; Messina, A.R.; Francois, B.; Bevrani, H. Optimal Energy Storage System-Based Virtual Inertia Placement: A Frequency Stability Point of View. *IEEE Trans. Power Syst.* **2020**, *35*, 4824–4835. [CrossRef]
47. Wang, S.; Yue, Y.; Cai, S.; Li, X.; Chen, C.; Zhao, H.; Li, T. A comprehensive survey of the application of swarm intelligent optimization algorithm in photovoltaic energy storage systems. *Sci. Rep.* **2024**, *14*, 17958. [CrossRef] [PubMed]
48. Almutairi, S.Z.; Alharbi, A.M.; Ali, Z.M.; Refaat, M.M.; Aleem, S.H.E.A. A hierarchical optimization approach to maximize hosting capacity for electric vehicles and renewable energy sources through demand response and transmission expansion planning. *Sci. Rep.* **2024**, *14*, 15765. [CrossRef] [PubMed]
49. Nikolaidis, P.; Poullikkas, A. Co-optimization of active power curtailment, load shedding and spinning reserve deficits through hybrid approach: Comparison of electrochemical storage technologies. *IET Renew. Power Gener.* **2022**, *16*, 92–104. [CrossRef]
50. Zhu, Y.; Liu, C.; Sun, K.; Shi, D.; Wang, Z. Optimization of Battery Energy Storage to Improve Power System Oscillation Damping. *IEEE Trans. Sustain. Energy* **2019**, *10*, 1015–1024. [CrossRef]

Disclaimer/Publisher's Note: The statements, opinions and data contained in all publications are solely those of the individual author(s) and contributor(s) and not of MDPI and/or the editor(s). MDPI and/or the editor(s) disclaim responsibility for any injury to people or property resulting from any ideas, methods, instructions or products referred to in the content.